THE JOURNAL OF BIOLOGICAL CHEMISTRY VOL. 284, NO. 7, pp. 4230–4237, February 13, 2009

Annular Protofibrils Are a Structurally and Functionally Distinct Type of Amyloid Oligomer*

Received for publication, November 12, 2008, and in revised form, December 18, 2008 Published, JBC Papers in Press, December 18, 2008, DOI 10.1074/jbc.M808591200

Rakez Kayed[‡1], Anna Pensalfini[‡], Larry Margol[‡], Yuri Sokolov[§], Floyd Sarsoza[¶], Elizabeth Head[¶], James Hall[§], and Charles Glabe[‡2]

From the [‡]Department of Molecular Biology and Biochemistry, [¶]Institute for Brain Aging and Dementia and Department of Neurology, and [§]Department of Physiology and Biophysics, University of California, Irvine, California 92697

Amyloid oligomers are believed to play causal roles in several types of amyloid-related neurodegenerative diseases. Several different types of amyloid oligomers have been reported that differ in morphology, size, or toxicity, raising the question of the pathological significance and structural relationships between different amyloid oligomers. Annular protofibrils (APFs) have been described in oligomer preparations of many different amyloidogenic proteins and peptides as ring-shaped or pore-like structures. They are interesting because their pore-like morphology is consistent with numerous reports of membrane-permeabilizing activity of amyloid oligomers. Here we report the preparation of relatively homogeneous preparations of APFs and an antiserum selective for APFs (αAPF) compared with prefibrillar oligomers (PFOs) and fibrils. PFOs appear to be precursors for APF formation, which form in high yield after exposure to a hydrophobic-hydrophilic interface. Surprisingly, preformed APFs do not permeabilize lipid bilayers, unlike the precursor PFOs. APFs display a conformation-dependent, generic epitope that is distinct from that of PFOs and amyloid fibrils. Incubation of PFOs with phospholipids vesicles results in a loss of PFO immunoreactivity with a corresponding increase in αAPF immunoreactivity, suggesting that lipid vesicles catalyze the conversion of PFOs into APFs. The annular anti-protofibril antibody also recognizes heptameric α-hemolysin pores, but not monomers, suggesting that the antibody recognizes an epitope that is specific for a β barrel structural motif.

Many age-related neurodegenerative diseases are characterized by the accumulation of amyloid deposits derived from a variety of misfolded proteins (1). These diseases typically have both sporadic and inherited forms, and in many cases the mutations associated with the familial forms are in the gene encoding the protein that accumulates or in genes directly related to its production, processing, or accumulation (2). The genetic linkage between the mutant allele and disease is evidence of the causal relationship of amyloid accumulation to pathogenesis, and many of the mutations either destabilize the natively folded state, produce more amyloidogenic protein, or they increase its propensity to aggregate (3). Although fibrillar amyloid deposits are among the most obvious pathognomonic features of disease, their role in pathogenesis is not clear. The extent of fibrillar amyloid plaque deposition does not correlate well with Alzheimer's disease pathogenesis, and there are a significant number of non-demented individuals that have equivalent amounts of amyloid plaques as disease patients (4). Pathological changes are observed in transgenic animals before the onset of amyloid plaque accumulation (5, 6), and it has been reported that soluble Aβ oligomers correlate better with dementia than insoluble, fibrillar deposits (7, 8), suggesting that oligomeric forms of Aβ may represent the primary toxic species. Soluble oligomers have been implicated as the primary toxic species in many degenerative diseases where the accumulation of large fibrillar deposits may be either inert, protective, or pathological by a different mechanism (for review, see Refs. 9 and 10).

Aβ aggregates have been described ranging in size from dimers up to particles of one million daltons or larger (11–16). In the atomic force microscope prefibrillar oligomers (PFOs)[3] appear as spherical particles of ~3–10 nm. PFOs appear at early times of incubation and disappear as mature fibrils appear (16–18). At longer times of incubation PFOs appear to coalesce to form curvilinear beaded strings that have been called protofibrils and ring-shaped, pore-like structures referred to as annular protofibrils (APFs) (17). APFs appear to be formed from the circularization of PFO subunits. A similar spectrum of PFOs and APFs has been observed for many types of amyloids, such as α-synuclein (19), islet amyloid (20), and non-disease associated "neoamyloids" (21). Although PFOs, APFs, and fibrils have been observed for many different types of amyloidogenic proteins and peptides (22), their structures, interrelationships, and contributions to disease pathogenesis are not entirely clear.

Insoluble fibrils and small soluble pieces of fibrils known as fibrillar oligomers appear to have a distinct and mutually exclusive underlying structure than PFOs because they display generic epitopes that are recognized by distinct conformation-dependent monoclonal antibodies (23, 24) and antisera (25, 26). It is not yet known whether APFs represent a unique conformation or whether they are structurally related to PFOs or

* This work was supported, in whole or in part, by National Institutes of Health Grants NS31230, AG16573, and AG00538. This work was also supported by the Cure Alzheimer Fund and The Larry L. Hillblom Foundation. The costs of publication of this article were defrayed in part by the payment of page charges. This article must therefore be hereby marked "*advertisement*" in accordance with 18 U.S.C. Section 1734 solely to indicate this fact.

[1] To whom correspondence should be addressed. Tel.: 949-824-6081; Fax: 949-824-8551; E-mail: cglabe@uci.edu.

[2] Present address: Dept. of Neurology, University of Texas, Medical Branch, Galveston, TX 77555.

[3] The abbreviations used are: PFO, prefibrillar oligomer; APF, annular protofibrils; αAPF, anti-APF; PFT, pore-forming toxin; MTT, (3-[4,5-dimethylthiazol-2-yl]-2,5-diphenyltetrazolium bromide; AD, Alzheimer disease; TBS-T, Tris-buffered saline-Tween; ELISA, enzyme-linked immunosorbent assay.

fibrils. So far APFs have only been defined morphologically as pore-like structures and have been observed in preparations of PFOs and in fibril-containing preparations (27–29). Familial mutations associated with inherited forms of Parkinson and Alzheimer diseases increase the formation of APFs, suggesting that their formation is related to pathogenic activity (17, 30). Based on the close resemblance between APFs and bacterial pore-forming toxins, it has been proposed that APFs permeabilize membranes (22). Because membrane permeabilization is a common pathogenic activity of prefibrillar amyloid oligomers (31) and PFOs are a precursor to annular protofibril formation, the formation of APFs is an attractive explanation for the membrane permeabilization of oligomers because annular protofibril formation is also a common assembly state and they resemble pores morphologically.

Investigating the pathological properties of Aβ APFs has been impeded by a lack of homogeneous preparations of annular structures and the lack of a facile means of distinguishing them from other aggregations states *in vivo*. Here we report the preparation of relatively homogeneous populations of APFs that have the same pore-like morphology previously described. We have used these preparations to examine their aggregation potential and membrane-permeabilizing properties and as an immunogen for the preparation of an antiserum that selectively recognizes APFs, compared with monomers, PFOs, and fibrils. APFs are stable and do not convert into fibrils or PFOs within months of incubation. APFs also exhibit much lower membrane-permeabilizing activity compared with the prefibrillar oligomer precursors to APF formation. Interaction with a hydrophobic-hydrophilic interface accelerates the conversion of PFOs into APFs. Incubation of PFOs with lipid vesicles results in a rapid loss of the prefibrillar oligomer specific epitope and the coordinate appearance of an annular protofibril-specific epitope. APFs display a unique conformation-dependent epitope that is distinct from PFOs and fibrils. Anti-annular protofibril antibody recognizes mature heptameric pores from α-hemolysin, suggesting that APFs may form β-barrel pore structures.

EXPERIMENTAL PROCEDURES

Aβ and islet amyloid polypeptide peptides were synthesized by fluoren-9-ylmethoxy carbonyl chemistry using a continuous flow semiautomatic instrument as described previously (11). α-Synuclein was a gift from Dr. Ralf Langen. α-Hemolysin (H9395) was obtained from Sigma.

Preparation and Characterization of APFs—Homogenous populations of annular (pore-like) protofibrils from different peptides and proteins was achieved by using PFOs as the starting material that were prepared as previously described (32). APFs were prepared by two different methods. PFOs were subjected to vigorous stirring in a 1.5-ml Eppendorf tube containing four 18-gauge needle holes in the cap to allow for slow evaporation of the water and subsequent exposure of spherical oligomers to air-water interface. Alternatively, 5% (v/v) of hexane was added to a solution of PFOs, and the sample was mixed with a vortex mixer for 1 min every 5 min for a total 50 min. Afterward the samples were dialyzed in water using a molecular mass cut-off membrane of 10 kDa.

The morphology of annular protofibril preparations was assessed by electron microscopy. 2 μl of the sample were adsorbed onto 200-mesh carbon and Formvar-coated grids, air-dried, and washed for 1 min in distilled water. The samples were negatively stained with 2% uranyl acetate (Ted Pella Inc., Redding, CA) for 2 min and viewed with a Zeiss 10CR microscope (80 kV). The thioflavin T binding properties of APFs was determined by adding 5-μl aliquots of each sample to a cuvette containing 145 μl of 3 μM thioflavin in 10 mM sodium phosphate buffer, pH 6.5 (33). For thioflavin, the fluorescence emission spectrum was measured in the range (465 mm– 600 nm) using a λ excitation at 442 nm. Fluorescence measurements were made with a Spex Fluorolog-2 spectrofluorometer.

Preparation and Specificity of Anti-annular Protofibril Antiserum—Homogenous populations of APFs from Aβ42 were prepared as described above. Rabbits were immunized under an approved animal protocol with 0.15 mg of Aβ42 APFs (dialyzed at 4 °C against phosphate-buffered saline, pH 7.6, overnight). For the first immunization equal parts of antigen and complete Freund's adjuvant were mixed together and used for immunization. Animals were injected subcutaneously at 5 sites in small increments of 0.1 ml per site in a checkerboard fashion on the scapular region. Booster immunizations were administered every 2 weeks using incomplete Freund's adjuvant. Serum was collected from the ear vein, allowed to clot, and centrifuged, and serum was frozen in aliquots.

The specificity of the anti-annular protofibril antiserum (αAPF) was tested with ELISA and dot blot and Western blot assays. For ELISA plates were coated with 50 ng of different amyloid aggregates (monomer, fibrils, PFOs, and APFs) using (0.1 M sodium bicarbonate, pH 9.6) as coating buffer, incubated for 1 h at 37 °C, washed 3 times with (Tris-buffered saline (TBS)-Tween), then blocked for 1 h at 37 °C with (10% bovine serum albumin, TBS-T). The bovine serum albumin was IgG-free (Sigma). The plates were then washed 3 times with (TBS-T), and 100 μl of αAPF antiserum (diluted 1:2000 in 5% nonfat milk in TBS-T) was added and allowed to react for 1 h at 37 °C. The plates were then washed 3 times with TBS-T, and 100 μl of horseradish peroxidase-conjugated anti-rabbit Ig (Promega) (diluted 1:10,000 in 5% nonfat milk in TBS-T) was added and incubated for 1 h at 37 °C. Finally, plates were washed 3 times with TBS-T and developed with 3,3′,5,5′-tetramethylbenzidine (TMB 1-component substrate) from KPL (Gaithersburg, MD). When the color developed, the reaction was stopped with 100 μl of 1 M HCl and read at 450 nm.

For dot blots, the 0.2-μg samples (prepared as described above) were applied as 1-μl spots to a nitrocellulose membrane, allowed to dry at room temperature, then blocked with 10% nonfat milk in TBS-T at room temperature for 1 h, washed 3 times for 5 min with TBS-T, and incubated for 1 h at room temperature with αAPF antiserum (IgG diluted 1:5000 in 5% nonfat milk in TBS-T or serum diluted 1:2000 in 5% nonfat milk in TBS-T). Membranes were washed 3 times for 5 min with TBS-T and incubated with horseradish peroxidase-conjugated anti-rabbit Ig (Promega) (1:10,000 in 5% nonfat milk in TBS-T incubated for 1 h at room temperature. Finally, membranes were washed three times with TBS-T and developed with ECL chemiluminescence kit from Amersham Biosciences.

For Western blots Aβ APFs were prepared at 0.2–0.3 mg/ml, and pore-forming toxins (PFTs) were prepared at 0.1 mg/ml in phosphate-buffered saline. Samples were mixed with an equal volume (10 μl) of 2× sample buffer just before loading and maintained at 25 °C. Samples were run on Criterion gels (Bio-Rad) and transferred to nitrocellulose. αAPF antibody was used for detection (diluted 1:2000) as described above for dot blots.

Membrane Permeabilization and Toxicity—Bilayers were formed at room temperature by the union of two monolayers as previously described (34, 35). Briefly, lipid monolayers were opposed over a hole ~150 μm in diameter in a 15-μm-thick Teflon partition dividing the two aqueous phases. The hole, punched by electric spark, was precoated with a 2.5% solution of squalene in *n*-pentane. Lipids were purchased from Avanti Polar Lipids (Birmingham, AL). Salt solutions contained 10 mM KCl buffered by 10 mM HEPES-Tris to pH 7.4. Solutions were stirred with magnetic stirring bars for about 30 s after the additions. Bilayer formation was monitored by measuring capacitance. Silver/silver chloride wires were used as electrodes to apply voltages and record currents across the bilayer. The rear chamber potential was taken as ground, and additions were made to the front chamber. Voltages were generated and currents were digitized at a resolution of 12 bits by a National Instruments PCI-6024E board (National Instruments, Austin, TX) controlled by JCLAMP (SciSoft Co., New Haven, CT). Currents were transduced by an Axopatch 200A amplifier (Axon Instruments, Foster City, CA).

Viability of neurons was assessed using the MTT colorimetric assay (Invitrogen) as previously described (25). Briefly, SH-SY5Y human neuroblastoma cells were treated with 2 μM Aβ APFs and PFOs. After incubation for 4 h at 37 °C, the cells were assayed using an MTT toxicity assay kit (Tox-1) (Sigma) according to the manufacturer's directions. All measurements were made in triplicate.

Immunohistological Localization of APF in AD Brain—Brain tissue samples were obtained from the Institute for Brain Aging and Dementia Tissue Repository. Two cases were used. The first was an 84-year-old female with a mini-mental state examination score of 30, 7 months before death. The post-mortem interval for this case was 4.3 h, and the final neuropathology diagnosis was normal (Braak and Braak stage III). The second case was a 79-year-old male with a mini-mental state examination score of 6, 9 months before death. The post-mortem interval for this case was 6 h, and the final neuropathology diagnosis was Alzheimer disease (Braak and Braak stage VI). The midfrontal gyrus was dissected from 4% paraformaldehyde-fixed coronal slices and sectioned at 50 μm using a Vibratome. Free-floating sections were stored in phosphate-buffered saline with 0.02% sodium azide before use in immunohistochemical or histology experiments. Sections were washed with 0.1 M TBS, pH 7.5, and then pretreated with 3% hydrogen peroxide in 10% methanol to block endogenous peroxidase activity. Pretreatment with 90% formic acid for 4 min did not affect subsequent immunostaining. Sections were subsequently washed in TBS with 0.1% Triton X-100 (TBS-A) and then blocked for 30 min TBS-A with 3% bovine serum albumin (TBS-B). Sections were incubated overnight at room temperature in several αAPF primary antibody dilutions (1:100–1:5000). After two washes with TBS-A and a wash in TBS-B, sections were incubated in goat anti-rabbit-biotinylated anti-IgG and then in avidin biotin complex (ABC) (Vector Laboratories, Burlingame, CA). Antibodies were visualized using 3,3′-diaminobenzidine (DAB, Vector Laboratories). Sections were counterstained with cresyl violet before coverslipping using Depex mounting media.

Liposome and Deoxycholate Treatment—Ten milligrams of phosphatidylcholines (Sigma) was dissolved in 500 μl of chloroform (20 mg/ml), the chloroform was evaporated under a stream of nitrogen in the hood, then the film was hydrated with 500 μl of buffer (10 mM HEPES, 100 mM NaCl, pH 7.4) and finally vortexed intensely for 3–5 min. Deoxycholate was used to promote oligomerization of α-hemolysin by incubating 6.25 mM α-hemolysin with 2 mg/ml deoxycholate at room temperature. Aβ42 oligomers were prepared at 66 μM in H_2O and incubated at room temperature with liposome in phosphate-buffered saline (1/10 (v/v) liposome/Aβ oligomers). For ELISA, plates were coated with 100 ng/well peptide or protein and detected with anti-oligomer antibody (A-11), 1:5,000, anti-annular protofibril antibody (αAPF) 1:5,000, and anti-rabbit 1:10,000.

RESULTS

Preparation and Properties of APFs—To examine the properties of Aβ APFs, we sought to establish reproducible methods for preparing them in relatively homogeneous populations. Because APFs are morphologically defined (17), we used electron microscopy to evaluate the morphological purity of samples. We noticed that samples of PFOs spontaneously contain APFs as previously reported and that exposure of these samples to an air-water interface during drying increased the abundance of annular structures observed (data not shown). We also examined the effect of treating solutions of Aβ42 spherical PFOs (Fig. 1*A*) with 5% hexanes in water and vortexing the two phase system. This procedure resulted in the formation of large numbers of relatively homogeneous annular structures (Fig. 1*B*). The APFs have diameters ranging from ~8 to 25 nm with a central opening or pore. When they are first formed, they appear to be made up of individual 3–5-nm spherical oligomeric subunits as previously reported. Upon further incubation for 7 days, the APFs lose this rough, beaded appearance and acquire a smooth appearance (Fig. 1*B*, *inset*). The APFs also appear to fuse at longer incubation times, giving rise to a lobular appearance. APFs of similar morphology, dimensions, and homogeneity were also obtained by the same methods with Aβ40 and α-synuclein (Fig. 1, *C* and *D*). No amyloid fibrils were observed by electron microscopy after incubation of APFs for up to 3 months either with or without seeding with fibrils, indicating that APFs are very stable and do not convert readily to fibrils under these conditions (data not shown). We also examined the secondary structure of APFs by circular dichroism spectroscopy (Fig. 1*E*). The spectrum demonstrates that APFs contain substantial β-sheet character.

Membrane Permeabilization Activity and Toxicity of APFs—Because APFs have a pore-like morphology and amyloid oligomers have been reported to permeabilize membranes, we examined the effect of APFs on membrane conductivity (Fig. 2). Surprisingly, APFs have little membrane-permeabilizing activ-

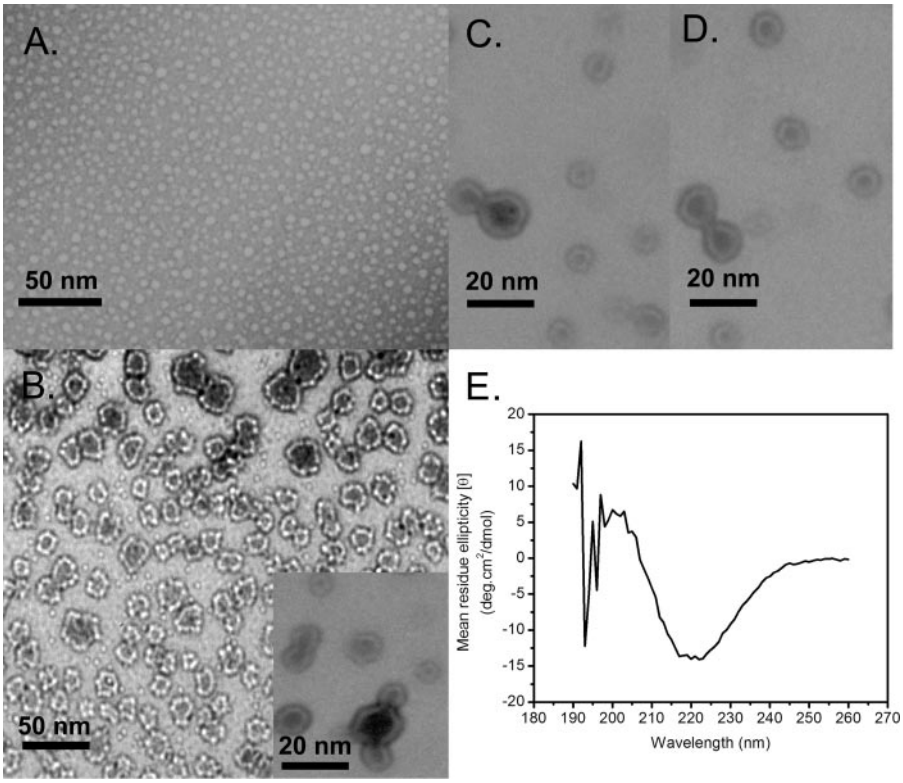

FIGURE 1. **Electron micrograph of PFOs and APFs and circular dichroism spectrum of APFs.** *A*, Aβ42 PFO preparation used as the starting material for APF preparation. *B*, Aβ42 APFs prepared by mixing with 5% hexanes appear as ring or pore-like structures of varying diameter from 8 to 25 nm. They are obtained in a relatively homogenous and pure population, although small amounts of 3–5-nm spherical oligomers are also observed in the population. Immediately after preparation, the APFs have a rough or beaded appearance that is 3–5 nm in diameter that suggests that APFs form by the coalescence of prefibrillar spherical oligomers as previously suggested. *Inset*, after incubation for 1 week at 25 °C, the APFs lose the rough, beaded appearance and become smooth. Figures that appear to result from the concatenation of multiple APFs are also observed. *C*, Aβ40 APFs after 1 week of incubation. *D*, α-synuclein APFs after 1 week of incubation. *E*, circular dichroism spectrum of APFs demonstrating the β-sheet character of APFs.

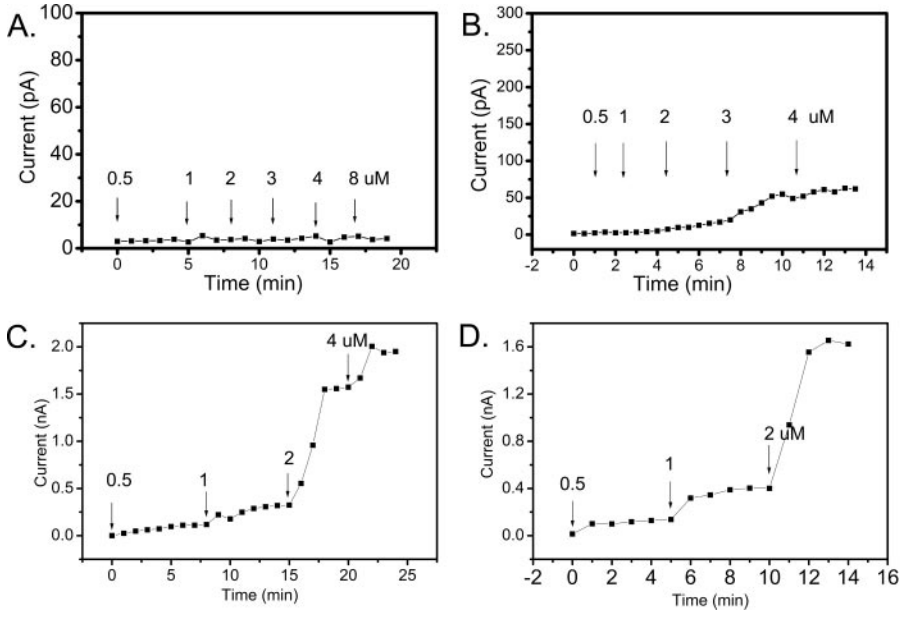

FIGURE 2. **Comparison of the effect of APFs and PFOs on the conductivity of black lipid membranes.** *A*, Aβ42 APFs. No significant change in conductivity was observed. *B*, α-synuclein annular protofibrils. A slight increase in conductivity was observed. *C*, Aβ42 PFOs. *D*, α-synuclein PFOs. *Arrows* indicate the time of addition of increasing amounts of APFs or PFOs at the final concentrations indicated. PFOs increase membrane conductivity in a concentration-dependent fashion.

ity compared with the PFOs that are used as precursors in annular protofibril formation. α-Synuclein APFs display weak permeabilizing activity with a conductivity of 40 pA at 4 μM (Fig. 2*B*), but this is much lower than the corresponding PFOs that give a conductivity of 1.2 nA at 2 μM (Fig. 2*D*). Because the annular protofibril preparations contain some residual PFOs (Fig. 1*A*), it is possible that the membrane-permeabilizing activity of the annular protofibril preparations may be due to contaminating PFOs rather than APFs. Recently a number of reports have shown that PFOs are more toxic than amyloid fibrils when applied exogenously to cells. We compared the toxicity of APFs and PFOs and found that the APFs are significantly less toxic (Fig. 3). Like the membrane-permeabilizing activity, the toxicity of APFs is less than that of the PFOs oligomers used to prepare them.

Anti-APF Antiserum—The different morphology and activity of APFs and PFOs suggests that there may be underlying conformational differences that account for these differences. We examined whether these differences could be recognized by conformation-dependent antibodies that are specific for these different structural motifs. We prepared antisera by immunizing rabbits with purified preparations of Aβ42 APFs and characterized the specificity of the serum for different aggregation states of Aβ and other amyloidogenic proteins and peptides by ELISA (Fig. 4). The anti-annular protofibril antisera (αAPF) selectively recognize annular protofibril preparations and display significantly less reactivity with monomeric and fibrillar samples. The αAPF serum also demonstrates some reactivity with prefibrillar oligomer samples, but it is not clear whether this represents shared epitopes or the fact that prefibrillar fibrillar oligomer preparations contain some spontaneously formed APFs. A11 and OC antisera recognize generic conformation-dependent epitopes that are widely distrib-

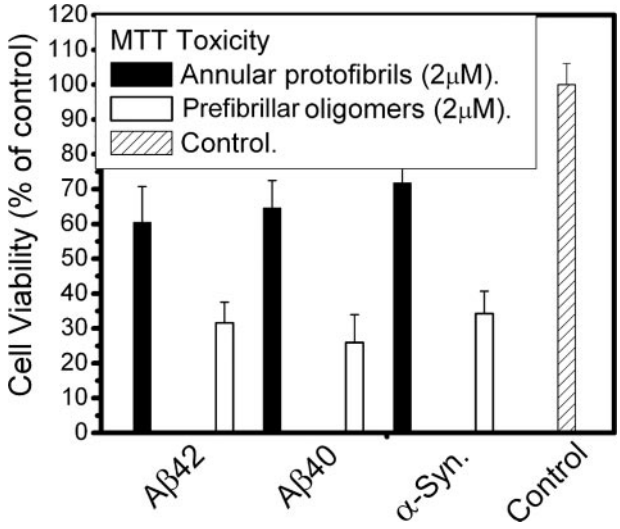

FIGURE 3. **Comparison of the toxicity of APFs and PFOs.** Cytotoxicity was measured using SHSY5Y cells and the MTT assay as described under "Experimental Procedures" using 2 μM APFs or PFOs. PFOs are significantly more toxic than APFs ($p < 0.05$).

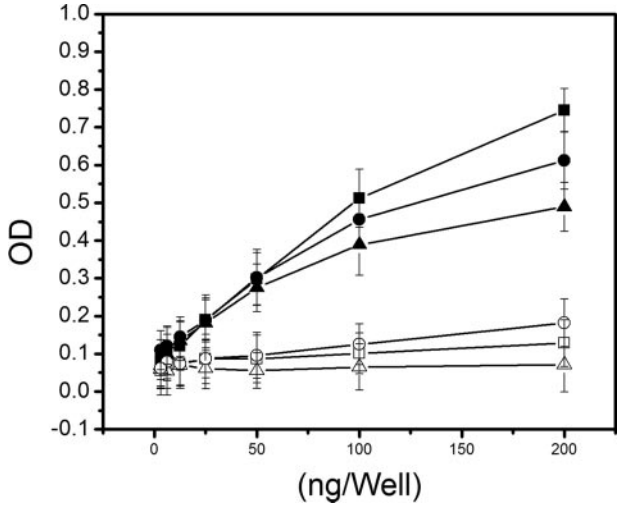

FIGURE 5. **αAPF antiserum recognizes conformation-dependent generic epitopes that are independent of specific amino acid sequences.** APFs and monomeric proteins and peptides were analyzed by ELISA for Aβ40 (■), islet amyloid polypeptide (●), and a-synuclein (▲). *Closed symbols*, APFs. *Open symbols*, monomeric proteins and peptides.

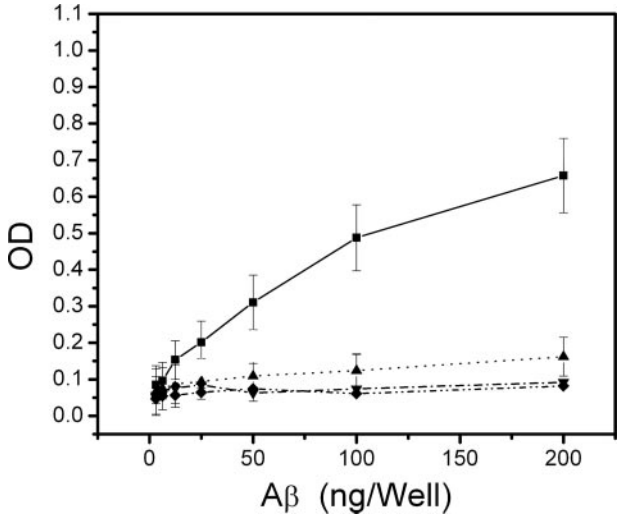

FIGURE 4. **Specificity of anti-annular protofibril antisera.** The immunoreactivity of the anti-annular protofibril antisera (anti-APF) was characterized by ELISA assay as described under "Experimental Procedures." Anti-APF antisera reacts selectively with APFs (■). Weak activity was observed with PFOs (▲). No reactivity is observed with monomers (♦) or fibrils (▼).

uted without regard to amino acid sequence, so we examined whether αAPF recognizes APFs from other protein and peptide sequences (Fig. 5). αAPF specifically recognizes APFs from α-synuclein and islet amyloid polypeptide and does not recognize the monomeric forms of these proteins, indicating that αAPF also recognizes generic epitopes.

We also compared the immunoreactivities of αAPF, A11, and OC antisera by dot blot analysis and Western blotting to test whether they have unique or overlapping specificities. Dot blots of monomer, APFs, PFOs, and fibrils reveal reactivity between PFOs, fibrils, and APFs with αAPF IgG (Fig. 6*A*). The reactivity of prefibrillar oligomer and fibril samples with αAPF may reflect overlapping immunoreactivities of the antisera or the difficulty of making pure samples of PFOs and fibrils *in vitro* that lack APFs. The latter is consistent with reports that APFs occur spontaneously in preparations of Aβ aggregates (17). However, annular protofibril samples are only weakly recognized by A11 anti-prefibrillar oligomer- and reactivity with OC anti-fibril antibody is undetectable. The weak A11 immunoreactivity is consistent with the interpretation that some spherical PFOs remain in preparations of APFs (Fig. 1*A*). The weak staining of prefibrillar oligomer and the lack of immunoreactivity of fibril samples with αAPF indicates that there is relatively little cross-reactivity or non-conformation-dependent immunoreactivity even though the antigens for all three antisera are different conformations of the same Aβ peptide sequence. Western blots of APFs reveal a band at ~55 kDa staining with αAPF that do not stain with either A11 or OC, indicating that APFs display an unique epitope that is not recognized by either A11 or OC (Fig. 6*B*). No staining of monomeric or low molecular weight aggregates is observed with αAPF. Because αAPF recognizes a unique epitope associated with APFs, we stained human AD brain tissue with αAPF antisera to examine its distribution in disease brain. No specific staining of either of two AD brain samples was observed, indicating that αAPF does not stain plaques and tangles that are characteristic features of disease (Fig. 7). This is further evidence that αAPF does not react with amyloid fibrils. We also examined lysates of six AD and four age-matched control brains and did not find any disease-related specific immunoreactivity (data not shown). These results are inconclusive regarding whether annular protofibrils exist *in vivo* because they may be below the limit of detection by these techniques.

Phospholipid Vesicles Promote APF Formation—Because drying at an air water interface or treatment with 5% hexane is artificial, we examined whether the conversion of PFOs to APFs could be accelerated under more physiological conditions. We investigated whether incubation with liposomes can catalyze this conversion using A11 and αAPF immunoreactivity as an assay for their conformational conversion. We found that incubation of PFOs with phosphatidylcholine

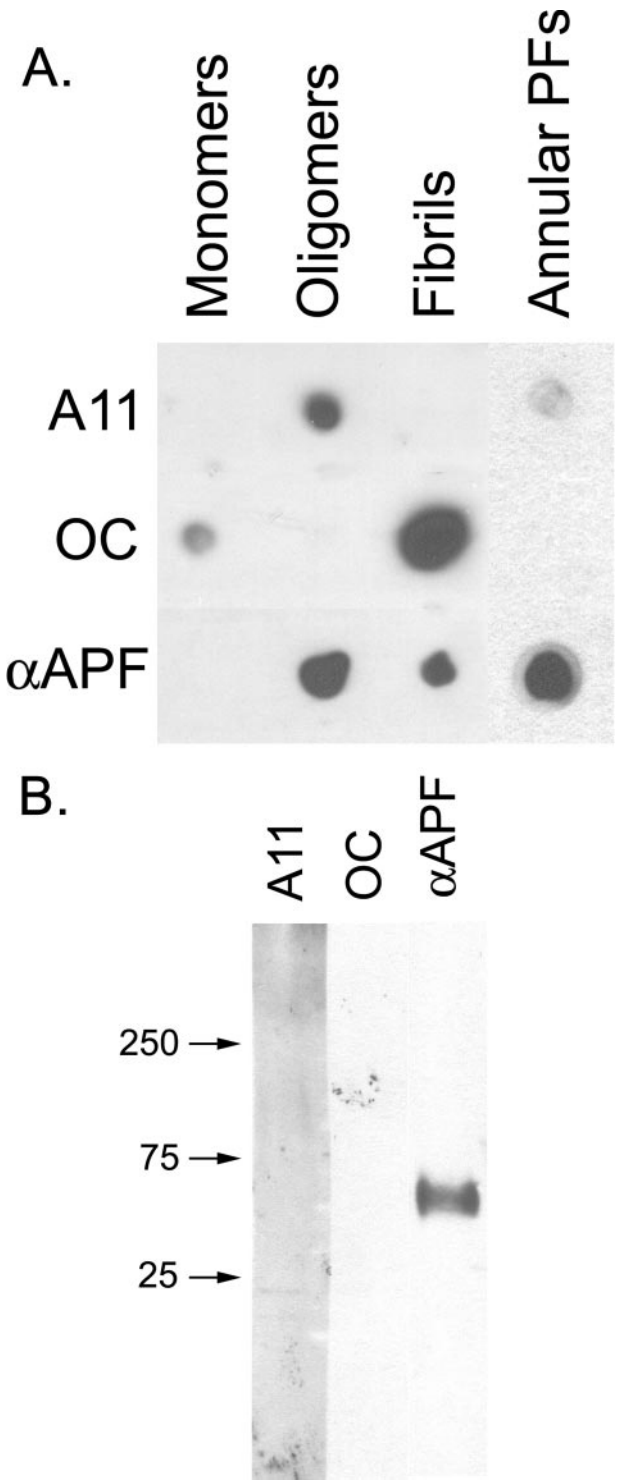

FIGURE 6. **αAPF recognizes an epitope specifically associated with APFs.** *A*, dot blot analysis of Aβ42 samples of monomer, PFOs, fibrils, and APFs with A11, OC, and αAPF. APFs are not stained by OC and only weakly stain with A11. *B*, Western blot analysis of Aβ42 APFs with A11, OC, and αAPF antibodies. αAPF specifically stains a band at ~60 kDa that is not recognized by A11 or OC.

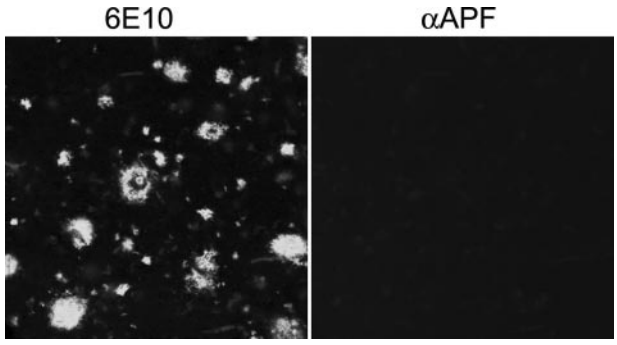

FIGURE 7. **αAPF fails to stain amyloid plaque deposits in AD brain.** 6E10 stains both compact and diffuse amyloid plaque deposits (*left panel*), whereas no specific staining of amyloid deposits was observed for αAPF (*right panel*). *Bar* = 20 μm.

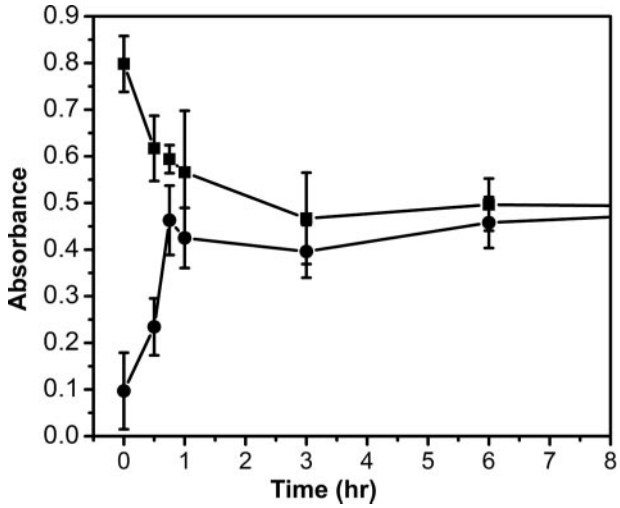

FIGURE 8. **Phosphatidylcholine vesicles catalyze the conformational conversion of PFOs to APFs.** A sample of 66 μM Aβ42 PFOs was mixed with 10 volumes of a solution of 25 mM phosphatidylcholine liposomes, and samples were taken at different times and analyzed by ELISA with A11 (■) or αAPF (●) antibodies. The loss of A11 immunoreactivity is correlated with an increase in αAPF reactivity.

liposomes greatly accelerates the loss of A11 immunoreactivity with a corresponding increase in αAPF immunoreactivity (Fig. 8). This indicates that PFOs can convert to APFs under more physiological conditions and suggests that the interaction of PFOs with membranes catalyzes their conformational conversion into annular protofibril pores, which may account for their ability to permeabilize membranes.

Anti-APF Antiserum Stains Heptameric Pores of α-Hemolysin—APFs morphologically resemble β-barrel pores that are assembled from bacterial PFTs. Like PFOs, pore-forming toxins assemble on target membranes by the conformation conversion of monomeric subunits into heptameric pores (36). We have previously reported that A11 intensely stains a partially unfolded protomeric intermediate of α-hemolysin and weakly stains the heptameric pore (37). We compared the staining of α-hemolysin pores, protomers and monomer with A11 and αAPF antibodies (Fig. 9*A*). In contrast to A11, αAPF antibody intensely stains the mature heptameric pore and only weakly stains the partially misfolded protomer band. Neither antibody stains the 33-kDa monomer band of α-hemolysin, indicating that the antibody recognition is conformation-dependent. Incubation of α-hemolysin with deoxycholate promotes pore formation and increases the αAPF staining of the heptameric pore band in a time-dependent fashion (Fig. 9*B*). This indicates that increasing αAPF immunoreactivity is promoted under more physiological conditions that may exist *in vivo*.

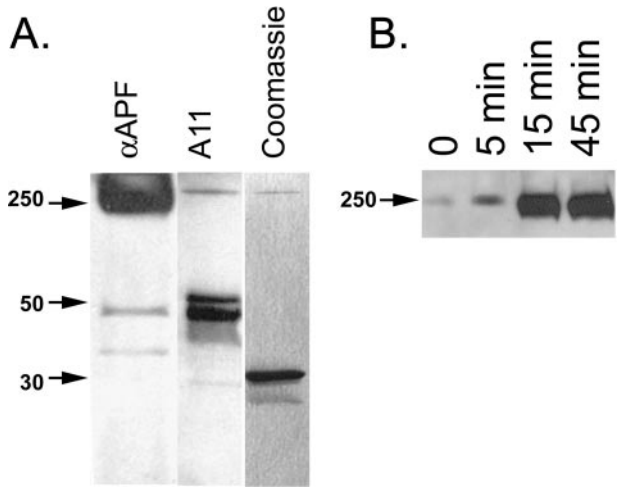

FIGURE 9. **αAPF stains heptameric α-hemolysin pores.** *A*, αAPF stains the mature pore band that runs at ~250 kDa and only weakly stains a partially misfolded protomer band at 48 kDa. In contrast, A11 weakly stains the mature pore and intensely stains the protomer bands. Neither antibody stains the 33-kDa monomer band which is the major species stained by Coomassie Blue. *B*, incubation of α-hemolysin with deoxycholate promotes the 250-kDa heptameric pores stained by αAPF in a time-dependent fashion.

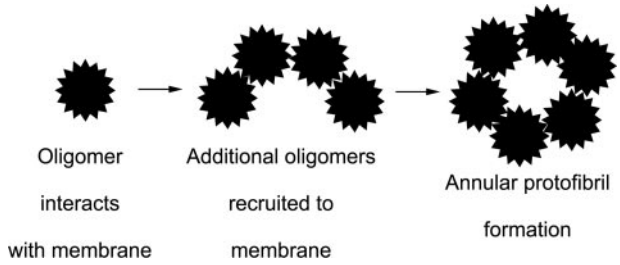

FIGURE 10. **Schematic diagram of annular protofibril formation at the surface of membranes.** PFOs interact with the membrane, which induces a conformation change giving rise to the αAPF epitope. Additional PFOs are recruited to the membrane surface. When a sufficient number of oligomers have adsorbed, the aggregates form a pore-like structure.

DISCUSSION

These results indicate that APFs represent a distinct class of amyloid oligomer that has a unique underlying structural motif that APFs from several types of amyloids share with bacterial PFTs. We discovered that relatively homogeneous populations of APFs are produced in response to exposure of PFOs to an air/water interface (slow drying with stirring) or a hydrophobic/hydrophilic (hexane/water) interface. This suggests that the structural rearrangement accompanying APF formation is driven by interfacial interactions of the amphipathic β-sheet. Although air/water and hexane/water interfaces are rather artificial, the same type of conformational conversion takes place upon incubation of PFOs with lipid bilayers. Because the interaction of PFOs with membranes leads to a loss of membrane permeability, this implies that the assembly of APFs on the surface of the bilayer may be a key event in the loss of membrane permeability (Fig. 10). Aβ amyloid oligomers are amphipathic and display micelle-like characteristics, like a critical concentration of assembly and a hydrophobic environment upon assembly (13). The stacked β sheets in amyloid fibrils also frequently display an amphipathic character where the interface between the two sheets excludes water (38). Amphipathic β sheets in amyloid oligomers may partition at the membrane bilayer polar/non-polar interface. As additional oligomers are recruited to the bilayer, they presumably hydrogen-bond with the other membrane-bound oligomers to form a β-barrel pore that integrates into the membrane in which the hydrophobic face of the bilayer faces the hydrocarbon core and the polar face forms a water-filled pore. A similar membrane-catalyzed assembly has been proposed for the bacterial PFTs in which the stepwise binding of toxin to the membrane, membrane-catalyzed conformation change, and toxin oligomerization leads to the formation of membrane embedded β-barrel pore (36).

Although the ring-like morphology of APFs is strikingly similar to membrane pores, we found that the annular protofibril preparations exhibit much lower membrane-permeabilizing activity than their corresponding PFO precursors. The toxicity of APFs is also reduced compared with PFOs but not as dramatically as the membrane-permeabilizing activity. This lack of membrane-permeabilizing activity of the preformed pore is similar to the lack of membrane permeabilization and hemolytic activity of preformed α-hemolysin pores (39). Mature pores purified from membranes aggregate in the absence of detergent and are incapable or re-inserting into the membrane. Perhaps the APFs, once formed, are incapable of inserting into the membrane and must assemble on the membrane.

The similarity of APFs and bacterial PFTs may include not only the ability to permeabilize membranes and the mechanisms of assembly but also structural similarity as well. We prepared a specific antiserum by immunizing rabbits with Aβ APFs. This serum displays a strong conformational preference for APFs compared with monomers, PFOs, and fibrils. When PFOs are incubated with lipid vesicles, the αAPF immunoreactivity increases in a time-dependent fashion, and the A11 immunoreactivity decreases coordinately, suggesting a precursor product relationship between the epitopes recognized by the two antibodies. Like the other conformation-dependent anti-amyloid antibodies we and others have described (23–26), the αAPF antisera recognizes a generic epitope that is largely independent of the specific amino acid sequence. Remarkably, the αAPF antisera also recognizes the heptameric α-hemolysin pores. The antibody binding is conformation-dependent because the monomeric α-hemolysin and the partially unfolded protomer are not stained with αAPF. These results suggest that the β-barrel pore is structurally related to APFs and that the αAPF antibodies recognize a unique backbone structure associated with β barrels.

We have previously reported that the α-hemolysin protomer is recognized by A11 anti-PFO antibody and that the heptameric pore is only weakly stained (37). The finding that A11 immunoreactivity is lost as αAPF increases upon treatment of PFOs with liposomes is consistent with a precursor-product relationship that is mechanistically similar to the relationship between the α-hemolysin protomer and its product, the heptameric pore. Indeed, treatments like deoxycholate, that are known to promote the conversion of α-hemolysin monomer to pores, increase αAPF immunoreactivity. The assembly of APFs on the membrane from PFO precursors can at least partially explain some of the discrepancy between reports of discrete pores by amyloids (40–42) and observations that PFOs permeabilize membranes efficiently without evidence of discrete, unitary conductances (34, 35). Preformed APFs would have a dis-

crete size and conductance, but they do not insert efficiently when they have been formed in the absence of the target membrane, like the heptameric hemolysin pore. In contrast, PFOs bind to the membrane and efficiently form APFs of varying size, which can explain why no discrete channels of unitary conductance are observed. Because PFTs have evolved to rapidly and efficiently permeabilize specific target membranes, they form heptameric pores with discrete, unitary conductances.

It has recently been demonstrated that phospholipids vesicles revert Aβ fibrils into A11 positive protofibrils or prefibrillar oligomers (43). Because phospholipids vesicles also catalyze the conversion of prefibrillar oligomers into annular protofibrils, this predicts that interaction with phospholipids could also cause the redistribution of amyloid fibrils to annular protofibrils. Although prefibrillar oligomers appear to be significantly more toxic *in vitro* (9, 25), the potential for lipid-induced conformational conversion complicates the interpretation of what is toxic *in situ*. The development of conformation-specific monoclonal antibodies that inhibit toxicity may help to resolve the question of which species is toxic *in situ*.

Taken together, these results suggest that APF toxicity is related to their ability to form membrane-permeabilizing β-barrel pores. β-Barrel pores are common in Gram-negative bacteria and the mitochondrial membrane, but otherwise they are rarely encountered in eukaryotes. The membrane attack complex/perforin proteins also form transmembrane β pores and, like their bacterial ancestors, permeabilize and lyse target cells (44, 45). Their activity is highly regulated, unlike APFs, which permeabilize membranes as a consequence of adopting a generic β structure. The relative absence of transmembrane β-barrels in eukaryotes may be a reflection of their generic toxicity and the difficulty in regulating it, suggesting that the motif has been selected against during evolution. The structural relationship between APFs and pore-forming toxins suggests that the ability to permeabilize membranes may be a common feature of amphipathic β barrels and that this property may represent a common mechanism of pathogenesis in amyloid-related degenerative diseases.

REFERENCES

1. Dobson, C. M. (2006) *Protein Pept. Lett.* **13,** 219–227
2. Hardy, J. (2005) *Biochem. Soc. Trans.* **33,** 578–581
3. Chiti, F., Stefani, M., Taddei, N., Ramponi, G., and Dobson, C. M. (2003) *Nature* **424,** 805–808
4. Terry, R. D. (1996) *J. Neuropathol. Exp. Neurol.* **55,** 1023–1025
5. Westerman, M. A., Cooper-Blacketer, D., Mariash, A., Kotilinek, L., Kawarabayashi, T., Younkin, L. H., Carlson, G. A., Younkin, S. G., and Ashe, K. H. (2002) *J. Neurosci.* **22,** 1858–1867
6. Billings, L. M., Oddo, S., Green, K. N., McGaugh, J. L., and Laferla, F. M. (2005) *Neuron* **45,** 675–688
7. McLean, C. A., Cherny, R. A., Fraser, F. W., Fuller, S. J., Smith, M. J., Beyreuther, K., Bush, A. I., and Masters, C. L. (1999) *Ann. Neurol.* **46,** 860–866
8. Lue, L. F., Kuo, Y. M., Roher, A. E., Brachova, L., Shen, Y., Sue, L., Beach, T., Kurth, J. H., Rydel, R. E., and Rogers, J. (1999) *Am. J. Pathol.* **155,** 853–862
9. Baglioni, S., Casamenti, F., Bucciantini, M., Luheshi, L. M., Taddei, N., Chiti, F., Dobson, C. M., and Stefani, M. (2006) *J. Neurosci.* **26,** 8160–8167
10. Haass, C., and Selkoe, D. J. (2007) *Nat. Rev. Mol. Cell Biol.* **8,** 101–112
11. Burdick, D., Soreghan, B., Kwon, M., Kosmoski, J., Knauer, M., Henschen, A., Yates, J., Cotman, C., and Glabe, C. (1992) *J. Biol. Chem.* **267,** 546–554
12. Hilbich, C., Kisters-Woike, B., Reed, J., Masters, C. L., and Beyreuther, K. (1991) *J. Mol. Biol.* **218,** 149–163
13. Soreghan, B., Kosmoski, J., and Glabe, C. (1994) *J. Biol. Chem.* **269,** 28551–28554
14. Garzon-Rodriguez, W., Sepulveda-Becerra, M., Milton, S., and Glabe, C. G. (1997) *J. Biol. Chem.* **272,** 21037–21044
15. Walsh, D. M., Lomakin, A., Benedek, G. B., Condron, M. M., and Teplow, D. B. (1997) *J. Biol. Chem.* **272,** 22364–22372
16. Harper, J. D., Wong, S. S., Lieber, C. M., and Lansbury, P. T. (1997) *Chem. Biol.* **4,** 119–125
17. Lashuel, H. A., Hartley, D., Petre, B. M., Walz, T., and Lansbury, P. T., Jr. (2002) *Nature* **418,** 291
18. Anguiano, M., Nowak, R. J., and Lansbury, P. T., Jr. (2002) *Biochemistry* **41,** 11338–11343
19. Conway, K. A., Harper, J. D., and Lansbury, P. T., Jr. (2000) *Biochemistry* **39,** 2552–2563
20. Janson, J., Ashley, R. H., Harrison, D., McIntyre, S., and Butler, P. C. (1999) *Diabetes* **48,** 491–498
21. Bucciantini, M., Giannoni, E., Chiti, F., Baroni, F., Formigli, L., Zurdo, J., Taddei, N., Ramponi, G., Dobson, C. M., and Stefani, M. (2002) *Nature* **416,** 507–511
22. Lashuel, H. A., and Lansbury, P. T., Jr. (2006) *Q. Rev. Biophys.* **39,** 167–201
23. Hrncic, R., Wall, J., Wolfenbarger, D. A., Murphy, C. L., Schell, M., Weiss, D. T., and Solomon, A. (2000) *Am. J. Pathol.* **157,** 1239–1246
24. O'Nuallain, B., and Wetzel, R. (2002) *Proc. Natl. Acad. Sci. U. S. A.* **99,** 1485–1490
25. Kayed, R., Head, E., Thompson, J. L., McIntire, T. M., Milton, S. C., Cotman, C. W., and Glabe, C. G. (2003) *Science* **300,** 486–489
26. Kayed, R., Head, E., Sarsoza, F., Saing, T., Cotman, C. W., Necula, M., Margol, L., Wu, J., Breydo, L., Thompson, J. L., Rasool, S., Gurlo, T., Butler, P., and Glabe, C. G. (2007) *Mol. Neurodegener.* **2,** 1–11
27. Hafner, J. H., Cheung, C. L., Woolley, A. T., and Lieber, C. M. (2001) *Prog. Biophys. Mol. Biol.* **77,** 73–110
28. Shtilerman, M. D., Ding, T. T., and Lansbury, P. T., Jr. (2002) *Biochemistry* **41,** 3855–3860
29. Ding, T. T., Lee, S. J., Rochet, J. C., and Lansbury, P. T., Jr. (2002) *Biochemistry* **41,** 10209–10217
30. Lashuel, H. A., Hartley, D. M., Petre, B. M., Wall, J. S., Simon, M. N., Walz, T., and Lansbury, P. T., Jr. (2003) *J. Mol. Biol.* **332,** 795–808
31. Glabe, C. G., and Kayed, R. (2006) *Neurology* **66,** Suppl 1, 74–78
32. Kayed, R., and Glabe, C. G. (2006) *Methods Enzymol.* **413,** 326–344
33. LeVine, H., III (1993) *Protein Sci.* **2,** 404–410
34. Kayed, R., Sokolov, Y., Edmonds, B., McIntire, T. M., Milton, S. C., Hall, J. E., and Glabe, C. G. (2004) *J. Biol. Chem.* **279,** 46363–46366
35. Sokolov, Y., Kozak, J. A., Kayed, R., Chanturiya, A., Glabe, C., and Hall, J. E. (2006) *J. Gen. Physiol.* **128,** 637–647
36. Montoya, M., and Gouaux, E. (2003) *Biochim. Biophys. Acta* **1609,** 19–27
37. Yoshiike, Y., Kayed, R., Milton, S. C., Takashima, A., and Glabe, C. G. (2007) *Neuromolecular Med.* **9,** 270–275
38. Sawaya, M. R., Sambashivan, S., Nelson, R., Ivanova, M. I., Sievers, S. A., Apostol, M. I., Thompson, M. J., Balbirnie, M., Wiltzius, J. J., McFarlane, H. T., Madsen, A. O., Riekel, C., and Eisenberg, D. (2007) *Nature* **447,** 453–457
39. Fussle, R., Bhakdi, S., Sziegoleit, A., Tranum-Jensen, J., Kranz, T., and Wellensiek, H. J. (1981) *J. Cell Biol.* **91,** 83–94
40. Arispe, N., Rojas, E., and Pollard, H. B. (1993) *Proc. Natl. Acad. Sci. U. S. A.* **90,** 567–571
41. Kagan, B. L., Azimov, R., and Azimova, R. (2004) *J. Membr. Biol.* **202,** 1–10
42. Lal, R., Lin, H., and Quist, A. P. (2007) *Biochim. Biophys. Acta* **1768,** 1966–1975
43. Martins, I. C., Kuperstein, I., Wilkinson, H., Maes, E., Vanbrabant, M., Jonckheere, W., Van Gelder, P., Hartmann, D., D'Hooge, R., De Strooper, B., Schymkowitz, J., and Rousseau, F. (2008) *EMBO J.* **27,** 224–233
44. Rosado, C. J., Buckle, A. M., Law, R. H., Butcher, R. E., Kan, W. T., Bird, C. H., Ung, K., Browne, K. A., Baran, K., Bashtannyk-Puhalovich, T. A., Faux, N. G., Wong, W., Porter, C. J., Pike, R. N., Ellisdon, A. M., Pearce, M. C., Bottomley, S. P., Emsley, J., Smith, A. I., Rossjohn, J., Hartland, E. L., Voskoboinik, I., Trapani, J. A., Bird, P. I., Dunstone, M. A., and Whisstock, J. C. (2007) *Science* **317,** 1548–1551
45. Hadders, M. A., Beringer, D. X., and Gros, P. (2007) *Science* **317,** 1552–1554